On proton charge radius definition

Trinhammer, Ole Lynnerup; Bohr, Henrik G.

Published in:
EPL

Link to article, DOI:
10.1209/0295-5075/128/21001

Publication date:
2019

Document Version
Publisher's PDF, also known as Version of record

LETTER

On proton charge radius definition

To cite this article: Ole L. Trinhammer and Henrik G. Bohr 2019 *EPL* **128** 21001

A Letters Journal Exploring the Frontiers of Physics

October 2019

EPL, **128** (2019) 21001
doi: 10.1209/0295-5075/128/21001

www.epljournal.org

On proton charge radius definition

Ole L. Trinhammer[1(a)] and Henrik G. Bohr[2]

[1] *Department of Physics, Technical University of Denmark - Fysikvej bld. 307, DK-2800 Kongens Lyngby, Denmark, EU*
[2] *Department of Chemical and Biochemical Engineering, Technical University of Denmark Søltofts Plads, bld. 229, DK-2800 Kongens Lyngby, Denmark, EU*

received 16 June 2019; accepted in final form 14 October 2019
published online 2 December 2019

PACS 14.20.Dh – Protons and neutrons

Abstract – We find a relation for the proton charge radius in closed form. The result 0.841235641(10) fm agrees with determinations from muonic hydrogen. Our relation is based on a mapping from an intrinsic configuration space for the proton to the observed size in laboratory experiments. The torus of the configuration space leads to periodic potentials in dynamical toroidal angles with the proton charge radius as a scale parameter in the mapping to laboratory space. The periodic potentials allow the introduction of Bloch phase factors which open for period doublings in the wave function. The opening of Bloch degrees of freedom is mediated by the Higgs mechanism. Thus, we find that pi times the proton charge radius equals twice the proton Compton wavelength.

Introduction. – The question of determining the proton charge radius has regained attention because of the slight, but significant discrepancy seen in experiments using muonic hydrogen $r_{\rm p}^{\mu} = 0.8409(4)\,\text{fm}$ [1–4] and experiments using electrons $r_{\rm p}^{\rm e} = 0.877(5)\,\text{fm}$ [5–7]. The corresponding values from the Particle Data Group are $r_{\rm p}^{\mu} = 0.84087(39)\,\text{fm}$ and $r_{\rm p}^{\rm e} = 0.8751(61)\,\text{fm}$, respectively [8]. Lately $r_{\rm p}^{\rm e}$ for electron scattering data is approaching $r_{\rm p}^{\mu}$ [9,10]. Other groups uphold similar roads to a solution [11,12]. However, a resolution of the puzzle through revised fit analyses has been criticized both for spectroscopic $r_{\rm p}^{\rm e}$ determinations [13] and $r_{\rm p}^{\rm e}$ determinations from scattering data [14]. For standard method reviews cf. [15,16]. These reviews describe the spectroscopic method and the scattering method. The spectroscopic method relies on the hydrogen Lamb shift which is sensitive to the electron, respectively the muon, wave function in the proton center due to their interaction with the quantized radiation field, cf. pp. 71 and 129 in [17]. With the heavier muon spending more time near the proton center, the muonic spectroscopic results are more accurate[1]. The scattering method is sensitive to the proton form factors which modify the differential scattering cross-section for point particle scattering, cf. p. 194 in [17]. The form factors are expanded in powers of the charge radius defined as moments of the proton charge density. Relativistically invariant moments for radius determination have recently been introduced from two-dimensional charge densities [18]. A variation of the scattering method is the MAMI initial state radiation (photon bremsstrahlung) experiment [19] which is sensitive to smaller momentum exchange and, therefore, potentially more accurate in form factor extraction for $r_{\rm p}^{\rm e}$ determination. Presently this method has not reached a level of accuracy compatible with muonic spectroscopy. The MAMI value is $(0.870 \pm 0.014_{\rm stat} \pm 0.024_{\rm sys} \pm 0.003_{\rm mod})\,\text{fm}$ and thus covers the muonic value within one standard deviation. For a future perpective on simultaneous electron and muon scattering on protons, cf. [20]. In the present work we find the following relation,

$$\pi r_{\rm p} = 2\lambda_{\rm p}, \tag{1}$$

between the proton charge radius r_p and the Compton wavelength $\lambda_{\rm p} \equiv h/(m_{\rm p}c)$ of the proton. The relation (1) derives from our description of the neutron decay and

(a) Corresponding author.

[1] Actually the value of the probability density at the center scales with the cube of the lepton mass, cf. p. 71 in [17].

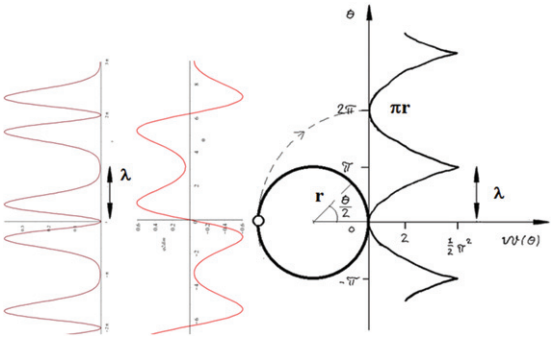

Fig. 1: The intrinsic space is shown with one toroidal dimension, the $U(1)$ circle. It is scaled by the proton radius r and mapped to the laboratory through a period doubled parametrization into the Compton wavelength λ for the proton. To the left is shown a period doubled 1D wave function which is part of the Slater determinant describing the intrinsic protonic state. To the far left is shown its square. The chopped harmonic oscillator graph to the right is a component of the intrinsic potential. The parametrization by $\theta/2$ reflects a Bloch phase factor $e^{i\theta/2}$ in the period doubled wave function. Figure and caption taken from [21].

yields $r_{\rm p} = 0.841235641(10)$ fm based on the experimental proton mass $m_{\rm p}$ [8] inserted via $\lambda_{\rm p}$ in (1) and it is in striking agreement with the result using muons. In particular we note the result $r_{\rm p} = 0.8412(15)$ fm using a higher-order determination of the muonic hydrogen Lamb shift [22]. Further experimental establishment of (1) would confirm the working of the Higgs mechanism in the neutron transformation to the proton [23].

As we shall see, the factor π in (1) originates in a toroidal structure from the intrinsic configuration space on which we describe the proton state. The factor two on the Compton wavelength originates in the period doubling involved in parametrizing the protonic state from the exterior laboratory space, cf. fig. 1. The present work is edited and updated from [21].

Intrinsic states. – As described in [24], we consider protons, neutrons and other baryons as stationary states on the intrinsic configuration space $U(3)$,

$$\frac{\hbar c}{a}\left[-\frac{1}{2}\Delta + \frac{1}{2}\mathrm{Tr}\ \chi^2\right]\Psi(u) = \mathcal{E}\Psi(u), \quad u = e^{i\chi} \in U(3). \tag{2}$$

In lattice gauge theory [25–29], u is a gluon plaquette variable and a is the lattice spacing. In the new interpretation used here, $u = e^{i\chi} \in U(3)$ is an intrinsic configuration variable for the entire baryonic state Ψ, $\hbar c/a \equiv \Lambda$ is an energy scale, Δ is the Laplacian and $\frac{1}{2}\mathrm{Tr}\ \chi^2$ is a representation independent and gauge invariant potential [28] depending only on the three eigenvalues $e^{i\theta_j}$ of u [30]. We call the dynamical variables $\theta_j, j = 1, 2, 3$ *eigenangles*. The potential is independent on left translations in configuration space because such translations correspond to conjugations $u \to vuv^{-1}$ to diagonalize u and leave the trace unchanged ($\mathrm{Tr}\ \chi^2 \equiv d^2(e,u) = d^2(v,vu) = d^2(e,vuv^{-1})$, for details cf. footnote 4 in [31]). This means that the potential is independent on the choice of *origo* e in configuration space. It can be shown that a left translation in configuration space corresponds to a (local) gauge transformation in laboratory space [23,32]. For a compact proof cf. [33]. The potential splits into a sum of three independent periodic terms in the eigenangles θ_j [30],

$$\frac{1}{2}\mathrm{Tr}\ \chi^2 = \sum_{j=1}^{3} w(\theta_j), \tag{3}$$

where (cf. fig. 1)

$$w(\theta) = \frac{1}{2}(\theta - n\cdot 2\pi)^2, \quad \theta \in [(2n-1)\pi, (2n+1)\pi],\ n \in \mathbb{Z}. \tag{4}$$

It may be interpreted as the Euclidean measure from the laboratory space folded onto the group manifold [34].

The configuration variable u can be excited from the laboratory space by nine kinematic generators. Thus,

$$\chi = (a\theta_j p_j + \alpha_j S_j + \beta_j M_j)/\hbar, \qquad \theta_j, \alpha_j, \beta_j \in \mathbb{R} \tag{5}$$

with intrinsic momentum generators

$$p_j = -i\frac{\hbar}{a}\frac{\partial}{\partial\theta_j}, \qquad j = 1, 2, 3 \tag{6}$$

and spin and Laplace-Runge-Lenz generators which in a coordinate representation (pp. 210 in [35]) spell out as, *e.g.*,

$$S_1 = a\theta_2 p_3 - a\theta_3 p_2 \quad \text{and} \quad M_1/\hbar = \theta_2\theta_3 + \frac{a^2}{\hbar^2}p_2 p_3. \tag{7}$$

The emergence of quarks from (2) is used in [24] to derive u and d parton distribution functions for the proton and described in more detail together with gluons in [23]. In [31] the generation of quark fields is also mentioned to yield the proton spin structure function and a relation between flavour and colour degrees of freedom is used to suggest an explanation for the value of the Cabibbo angle. The potential (3) is a Manton analogue [28] of the Wilson trace here used on the configuration variable u [25,27],

$$V_{\rm Wilson}(u) = \frac{1}{2}\mathrm{Tr}(2I - (u + u^\dagger)). \tag{8}$$

The two expressions (3) and (8) are compared in fig. 2. The Laplacian Δ can be written in a polar decomposition [36]

$$\Delta = \sum_{j=1}^{3}\frac{1}{J^2}\frac{\partial}{\partial\theta_j}J^2\frac{\partial}{\partial\theta_j} - \frac{1}{\hbar^2}\sum_{\substack{i<j\\ k\neq i,j}}^{3}\frac{S_k^2 + M_k^2}{8\sin^2\frac{1}{2}(\theta_i - \theta_j)}, \tag{9}$$

where $e^{i\theta_j}$ are the three eigenvalues of u in a 3×3 matrix representation and θ_j are dynamical *eigenangles* with action-angle quantization conditions

$$\left[\frac{\partial}{\partial\theta_i}, \theta_j\right] = \delta_{ij}. \tag{10}$$

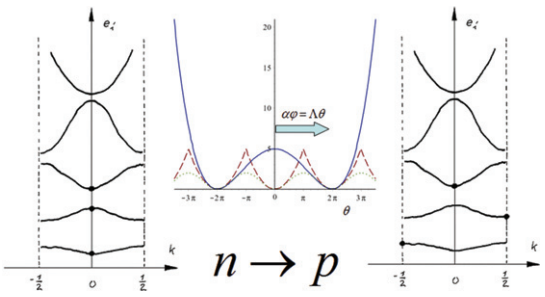

Fig. 2: Left and right: reduced zone schemes (cf. p. 160 in [37]) for Bloch wave numbers for the neutron state (left) and the proton state (right). The band widths of lower levels are grossly exaggerated for clarity. Middle: Higgs potential (solid line) matching the Manton-inspired potential [28] (dashed line) and the Wilson-inspired potential [25] (dotted line). The Manton and Wilson-inspired potentials yield the same value for the Higgs mass and the electroweak energy scale, whereas only the Manton-inspired potential gives a satisfactory reproduction of the baryon spectrum [23,32]. Figure adapted from [38].

The polar decomposition is analogous to the Euclidean Laplacian in polar coordinates

$$\Delta_{e,polar} = \frac{1}{r^2}\frac{\partial}{\partial r}r^2\frac{\partial}{\partial r} - \frac{1}{r^2}\mathbf{L}^2, \tag{11}$$

for instance used in solving the hydrogen atom. The "Jacobian" of the parametrization in (9) is (cf. p. 197 in [39])

$$J = \prod_{i<j}^{3} 2\sin\left(\frac{1}{2}(\theta_i - \theta_j)\right) \tag{12}$$

and S_k and M_k are off-toroidal generators equivalent to off-diagonal Gell-Mann matrices, cf. p. 210 in [35],

$$[M_k, M_l] = [S_k, S_l] = -i\hbar\epsilon_{klm}S_m \tag{13}$$

carrying spin and flavour degrees of freedom, respectively. The Laplacian (9) in its polar form matches the potential (3) since the trace expression only depends on the eigenvalues $e^{i\theta_j}$ of the configuration variable. Due to the match in the parametrization of the Laplacian and the potential, the wave function factorizes into

$$\Psi(u) = \tau(\theta_1, \theta_2, \theta_3)\Upsilon(\alpha_1, \alpha_2, \alpha_3, \beta_1, \beta_2, \beta_3). \tag{14}$$

To solve (2), we first differentiate through J^2 in (9), then multiply by J and finally integrate out the six off-toroidal degrees of freedom $\alpha_1, \alpha_2, \alpha_3, \beta_1, \beta_2, \beta_3$ to obtain a dimensionless equation for the toroidal part $R \equiv J\tau$ of the measure-scaled wave function $\Phi \equiv J\Psi$ [24],

$$\left[-\frac{1}{2}\sum_{j=1}^{3}\frac{\partial^2}{\partial\theta_j^2} + W\right]R(\theta_1, \theta_2, \theta_3) = \mathrm{E}R(\theta_1, \theta_2, \theta_3). \tag{15}$$

Here $\mathrm{E} = \mathcal{E}/\Lambda$ and

$$W = -1 + \frac{1}{2}\cdot\frac{4}{3}\sum_{i<j}^{3}\frac{1}{8\sin^2\frac{1}{2}(\theta_i - \theta_j)} + \sum_{j=1}^{3}w(\theta_j). \tag{16}$$

The nominator 4 in (16) is the minimum value of $(\mathbf{S}^2 + \mathbf{M}^2)/\hbar^2$ [23,24]. The eigenvalues of (15) with the potential (16) yields the N and Δ baryon resonance spectrum with no serious missing resonance problem, cf. [23,32].

To solve (15) by a Rayleigh-Ritz method [40] for period doubled states, we may expand R on Slater determinants,

$$b_{pqr} = \begin{vmatrix} e^{-i\frac{\theta_1}{2}}\cos p\theta_1 & e^{-i\frac{\theta_2}{2}}\cos p\theta_2 & e^{-i\frac{\theta_3}{2}}\cos p\theta_3 \\ \sin\left(q-\frac{1}{2}\right)\theta_1 & \sin\left(q-\frac{1}{2}\right)\theta_2 & \sin\left(q-\frac{1}{2}\right)\theta_3 \\ e^{-i\frac{\theta_1}{2}}\cos r\theta_1 & e^{-i\frac{\theta_2}{2}}\cos r\theta_2 & e^{-i\frac{\theta_3}{2}}\cos r\theta_3 \end{vmatrix}. \tag{17}$$

We have not restricted the set of integers p, q, r to make $\{b_{pqr}\}$ a complete set and, therefore, we know only approximate solutions with $p = 0, 1, \ldots, P-1$; $q = 1, 2, \ldots, P$; $r = p+1,\ p+2, \ldots, P$. Work is in progress on this[2]. *However, the point of interest here for the proton radius is the fact that for all terms in the expansion of R, the parametrizations via the θ_j's in (17) introduce a period doubling.*

What is the origin of the period doublings? They come from exploiting the Higgs mechanism in the neutron decay to lower the eigenvalue of the intrinsic baryonic state from that of the neutron to that of the proton. The mechanism is summed up in fig. 2.

Period doubling and proton radius. – The periodic potential W in (16) calls for a description with concepts from solid-state physics where periodic potentials offer Bloch degrees of freedom. In our case the wave function needs to have single-valued square on the configuration space. This selects Bloch phase factors $e^{i\kappa\theta}$ with $\kappa = 0, \pm\frac{1}{2}$. Choosing $\kappa = 0$ gives neutronic states, whereas $\kappa = \pm\frac{1}{2}$ introduces a topological winding and lowers the energy as seen to the right in fig. 2. We interpret the topological change as the creation of electric charge in the decay

$$n \to p + e + \overline{\nu}_e. \tag{18}$$

To allow the period doubling we invoked the Higgs mechanism [23]. The Higgs mechanism is normally presented in the lepton sector as the agent behind the spontaneous breakdown of the $U(2)$ symmetry of a leptonic doublet,

$$\left\{\begin{array}{c}\nu_{\mathrm{e}}\\ e\end{array}\right\} \to \left\{\begin{array}{c}\nu_{\mathrm{e}}\\ e\end{array}\right\}_L, \quad e_R, \quad \nu_{\mathrm{e},R}, \tag{19}$$

into a chirally broken $SU(2)$ symmetry times a remaining $U(1)$ symmetry providing three massive gauge bosons $W^{\pm}, Z^0$ and a massless photon. But *the same symmetry breakdown* happens for the electroweak degrees of freedom of the quarks in hadrons, cf. pp. 378–379 in [42] and p. 240 in [43]. For instance the up and down flavour quarks are also thought to break up into right-handed $SU(2)$-singlets

[2] Cf. appendix A.4.1 in [41] for restrictions on p, q, r in a 3D exponential base in the text p. 181 following eq. (A.119).

and a left-handed doublet,

$$\left\{ \begin{array}{c} u \\ d \end{array} \right\}_L \sim \left\{ \begin{array}{c} \nu_{\rm e} \\ e \end{array} \right\}_L . \tag{20}$$

Quarks have both colour characteristics for strong interactions and flavour for electroweak interactions and we take the similarity in (20) to support a relation among strong and electroweak degrees of freedom. We make the following trailing Ansatz to correlate the sectors:

$$\Lambda\theta = \alpha\varphi. \tag{21}$$

Here Λ and α scale the trailing among the colour angle field θ and the scalar Higgs field φ. We found the Higgs field vacuum expectation value φ_0 by the 2π shift from one trough to a neighbouring one in the periodic potential (4), cf. fig. 2,

$$\Lambda 2\pi = \alpha\varphi_0. \tag{22}$$

The shift corresponds to the exchange of one quantum of action h between the two sectors[3].

Higgs potential and electroweak scale. – We fitted the Higgs potential to the periodic potential (4) as seen in fig. 2 and found [23]

$$V_{\rm H}(\phi) = \frac{1}{2}\delta^2\varphi_0^2 - \frac{1}{2}\mu^2(\phi^\dagger\phi) + \frac{1}{4}\lambda^2(\phi^\dagger\phi)^2, \tag{23}$$
$$\delta^2 = \frac{1}{4}\varphi_0^2, \quad \mu^2 = \frac{1}{2}\varphi_0^2, \quad \lambda^2 = \frac{1}{2}, \quad \varphi_0 = \frac{2\pi}{\alpha}\Lambda.$$

From this there follows $m_{\rm H}c^2 = \frac{1}{\sqrt{2}}\varphi_0$. The 2π shift sets the electroweak energy scale v to

$$\frac{v}{\sqrt{2}} = \varphi_0 = \frac{2\pi}{\alpha}\Lambda. \tag{24}$$

Note that the standard model value $v_{\rm SM}$ is related to our v by the u and d quark mixing matrix element V_{ud}, thus $v_{\rm SM} = v\sqrt{|V_{ud}|}$ [23,44]. From the Higgs potential and the scale (24) we got an accurate expression for the Higgs mass [23,38] the value of which we update here:

$$m_{\rm H}c^2 = \frac{1}{\sqrt{2}}\frac{2\pi}{\alpha(m_{\rm W})}\frac{\pi}{\alpha_{\rm e}}m_{\rm e}c^2 = 125.095 \pm 0.014\,{\rm GeV}. \tag{25}$$

The fine-structure couplings are $\alpha(m_{\rm W}) = 1/127.989(14)$ (see footnote [4]) at the W boson scale [38] and $\alpha_{\rm e} = 1/137.035999139(31)$ at the electron scale [8], respectively. The electron mass enters from our use of the classical electron radius, cf. [46] and p. 97 in [47],

$$r_{\rm e} = \frac{e^2}{4\pi\epsilon_0 m_{\rm e}c^2} \tag{26}$$

to set the length scale a in (2) by the projection relation, cf. fig. 3 [24],

$$\pi a = r_{\rm e}. \tag{27}$$

This projection rests on the existence of a map from the intrinsic torus to space coordinates, thus

$$x_j = a\theta_j. \tag{28}$$

The choice of $r_{\rm e}$ in (27) to set the exterior scale in mapping the intrinsic scale is heuristically motivated by the fact that the electron with its rest mass $m_{\rm e}$ is created simultaneously with the topological change giving p its charge in the transformation from the neutral neutron n to the charged p. We have called the electon a "peel-off" [24] and we have described the proton as "charge scarred". The scale introduced in (26) led to an accurate value for the electron-to-neutron mass ratio [24]

$$\frac{m_{\rm e}}{m_{\rm n}} = \frac{\alpha(m_{\rm n})}{\pi}\frac{1}{{\rm E}_{\rm n}} = \frac{1}{1839(1)}, \tag{29}$$

where the fine structure coupling is to be taken at nucleonic energies. The same scale is to be used for the baryon spectra. Cf. [23,32] for approximate solutions for charged states. The result in (29) is calculated with $\alpha^{-1}(m_{\rm n}) = 133.61$ obtained by sliding with radiative corrections from $\alpha^{-1}(m_\tau) = 133.476(7)$ [8] and with ${\rm E}_{\rm n} = \mathcal{E}_{\rm n}/\Lambda = 4.382(2)$

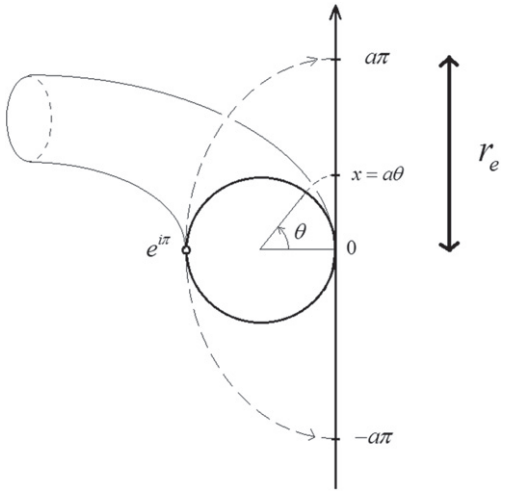

Fig. 3: A projection from a toroidal degree of freedom (the $U(1)$ circle) of the intrinsic configuration space used in our description of the neutron transformation in the neutron decay. We use the classical electron radius $r_{\rm e}$ [46,47] to set the length scale a for the projection of the intrinsic dynamics. Figure taken from [23].

[3] First introduce a time projection $a\theta_0 = ict$ [41] in analogy with our space projection (28). Then we have a time interval τ for a full period given by $a2\pi = c\tau$. Second consider the exchange of one quantum of action h during the time τ, thus $\Lambda\tau = h$ or $\Lambda c\tau = hc$ where we introduce hc as a *quantum of space action* to get $\alpha\varphi_0 a = hc$ for the quantum exchange with the Higgs field. Equating the two space quanta within the full period leads to (22).

[4] Here we use $m_{\rm u} = 0.0022\,{\rm GeV}$ and $m_{\rm d} = 0.0047\,{\rm GeV}$ and so on from [8] for sliding from $\alpha(m_{\rm Z})$ to $\alpha(m_{\rm W})$. The value $m_{\rm H}c^2 = (125.095 \pm 0.010\alpha(m_{\rm Z}) \pm 0.0003(n_{\rm f}) \pm 0.00003(\alpha_{\rm s}) \pm 0.003(m_{\rm q}) \pm 0.00014(m_{\rm Z,W}))\,{\rm GeV}$ in (25) compares extremely well with both $(125.18 \pm 0.16)\,{\rm GeV}$ from [8] and with the present world average $m_{\rm H}c^2 = (125.10 \pm 0.14)\,{\rm GeV}$ [45].

where $\mathcal{E}_\mathrm{n}$ is the neutron ground-state eigenvalue found in a Rayleigh-Ritz solution [38] of (15) with 3078 base functions [23]. With $r_\mathrm{e} = e^2/(4\pi\epsilon_0 m_\mathrm{e}c^2)$ eq. (27) gives $a = 0.92\ldots$ fm for the length scale used in the space projection (28) of the toroidal angles in the neutronic state.

Proton charge as topological. – After the neutron decay the emerging proton lives in laboratory space as an extended charge-scarred object. Being a quantum object it will have "fuzzy edges", with an extension conventionally described by its Compton wavelength

$$\lambda_\mathrm{p} = \frac{h}{m_\mathrm{p}c}. \tag{30}$$

This wavelength is an experimentally observable quantity, *e.g.*, in Compton scattering. For a lucid description of Compton scattering of photons off electrons cf. p. 6 in [48]. The photon, in its role of being the $U(1)$ gauge field of electromagnetism, interacts with the electric charge. We therefore take the Compton wavelength λ_p to be the projected extension in laboratory space relating to the charge of the proton. We are aware that the Compton wavelength is defined also for neutral particles and is determined by the mass of the particle. We come to this more general conception in the next section. The length scale to be used in the mapping of the *intrinsic* charge scar we will identify as the proton charge radius r_p. We do not want to imply that it would mean that the proton as a space object has a sharp, well-defined radius. Rather as stated, the radius is a scale parameter for a mapping analogous to the one in (28). Now, as the mapping of the intrinsic protonic state has to take into account the period doubling from the Bloch phase factors $e^{i\theta/2}$ in (17), the projectional relation analogous to (28) reads

$$x_j = r_\mathrm{p}\frac{\theta_j}{2} \tag{31}$$

or, for a full extension projection,

$$\lambda_\mathrm{p} = r_\mathrm{p}\frac{\pi}{2}, \tag{32}$$

as shown in fig. 1 and equivalent to eq. (1),

$$\pi r_\mathrm{p} = 2\lambda_\mathrm{p}.$$

The result for r_p is

$$r_\mathrm{p} = 0.841235641(10)\,\mathrm{fm} \tag{33}$$

in agreement with the root-mean-square value of the proton charge distribution [8]

$$r_\mathrm{p}^\mu = \langle r^2\rangle^{\frac{1}{2}} = 0.84087(39)\,\mathrm{fm} \tag{34}$$

as observed by spectroscopy on muonic hydrogen [1,3,4]. The uncertainty in (33) is from the experimental uncertainty on the proton mass m_p and Planck's constant h, both known with a relative uncertainty of $6\cdot 10^{-9}$. That is, we use $m_\mathrm{p}c^2 = 938.272081(6)\,\mathrm{MeV}$ and $\hbar c = 197.3269788(12)\,\mathrm{MeV\,fm}$ [8]. Allowing for a possible systematic correlation among the two uncertainties, the uncertainty we cite in (33) is a conservative estimate from summing the relative uncertainties instead of combining them independently in quadrature.

The relation (32) for the proton charge radius does not depend on any approximation. It solely depends on the topological *structure* of the wave function, *i.e.*, on the fractional Bloch phase factors from eq. (17) manifested in the fraction $\frac{1}{2}$ in (32) —and signifying the creation of the proton charge. Note that the same kind of period doublings lie behind the approximate protonic state from which parton distribution functions were generated in ref. [24].

Mass as intrinsic energy-momentum. – We here connect our relation (32) to semi-classical considerations. We start out by the diffential geometry underlying the treatment of (2). From the compactness of the intrinsic configuration space $U(3)$ and the exchange of energy-momentum through the exterior derivatives (momentum forms) $\mathrm{d}R$ and $\mathrm{d}\Phi$ operating on the intrinsic wave function we get an intuitive conception of baryonic massiveness as *introtangled* energy-momentum. The exterior derivatives act on the momentum generators and rotation generators in laboratory space and thereby map the intrinsic wave function to laboratory space. In particular, by the projection of the toroidal degrees of freedom [24] on the spatial degrees of freedom (28), we imagine the extension of a baryon as a compromise on the impossibility of point-like localization and mutual, definite "curled up" momentum [49]. We take the general relation

$$\mathcal{E}^2 = p^2c^2 + m^2c^4 \tag{35}$$

among energy $\mathcal{E}$, momentum p and mass m as defined in spacetime where c is the velocity of pure energy configurations and assume formally that intrinsic dynamics is that of pure energy (zero mass and no gravity in intrinsic space). Then from an intrinsic point of view

$$\mathcal{E}^2 = p_\mathrm{int}^2c^2. \tag{36}$$

In the complementary real-space configuration, the state is a particle at rest (zero momentum), so we have

$$\mathcal{E}^2 = m^2c^4. \tag{37}$$

The right-hand sides of (36) and (37) are squares of corresponding eigenvalues for the same baryonic entity in (2) only seen from complementary spaces. Thus,

$$p_\mathrm{int}c = mc^2. \tag{38}$$

With the quantization inherent in the concept of the de Broglie wavelength and the Bohr-Sommerfeld quantization condition for the action integral $\oint p\,\mathrm{d}q = nh, n\in\mathbb{Z}^+$ (cf. p. 36 in [50]) we infer for $n = 1$

$$p_\mathrm{int}\lambda_0 = h \to \lambda_0 = \frac{h}{mc} = 2\pi\frac{\hbar c}{\mathrm{E}\Lambda} = \frac{2\pi a}{\mathrm{E}}. \tag{39}$$

The fourth expression is the Compton wavelength of the particle as conceived in real space. The last expression opens for relating the proton charge radius in (1) to the classical electron radius by using $\pi a = r_{\rm e}$ from (27) in (39) to yield

$$r_{\rm p} = \frac{4}{\pi {\rm E}} \frac{\alpha(m_{\rm n})}{\alpha_{\rm e}} r_{\rm e} = 0.8398(4)\,{\rm fm}. \tag{40}$$

Here the main uncertainties lie in ${\rm E} = 4.382(2)$ determined from (15) and in the necessary sliding from the fine-structure coupling $\alpha^{-1}(m_\tau) = 133.476(7)$ at tauonic energies [8] to nucleonic energies in the neutron-to-proton transformation where $\alpha^{-1}(m_{\rm n}) = 133.61(1)$. This has only been done for radiative corrections and not for fermionic corrections since here we are outside the pertubative regime of QCD. We may insert the classical electron radius (26) in (40) to get

$$r_{\rm p} = \frac{4}{\pi {\rm E}} \frac{\alpha(m_{\rm n})}{\alpha_{\rm e}} \frac{e^2}{4\pi\epsilon_0 m_{\rm e} c^2} = \frac{4\,\alpha(m_{\rm n})}{\pi {\rm E}} \frac{\hbar c}{m_{\rm e} c^2}, \tag{41}$$

where the last expression involves the proton charge in the fine-structure coupling at nucleonic energies.

Conclusion. – We have defined a proton charge radius from a conception of the proton structure based on a Hamiltonian on the intrinsic configuration space, the Lie group $U(3)$. The compactness of the intrinsic space manifests itself in parameter space as periodic potentials. The periodic potentials open for Bloch phase factors allowing period doublings with topological consequences in the wave function of the proton relative to that of the neutron thereby lowering the nucleon ground state. Our result relates the proton charge radius to its Compton wavelength and the result is in excellent agreement with experimental results using spectroscopy on muonic hydrogen. Further confirmation of our result would stress the connection between the period doublings and the Higgs mechanism which opens the necessary degrees of freedom. We look forward to results from simultaneous electron and muon scattering on protons.

* * *

We thank The Technical University of Denmark for the institutional framework. We thank Thomas Lyspil for an observation on the Rydberg constant. In particular we thank our colleague Mogens Stibius Jensen for co-work on the Higgs mass.

REFERENCES

[1] Pohl R. *et al.*, *Nature*, **466** (2010) 213.
[2] Margolis H. S., *Science*, **339** (2013) 405.
[3] Antognini A. *et al.*, *Science*, **339** (2013) 417.
[4] Antognini A. for the CREMA Collaboration, *Muonic atoms and the nuclear structure*, *ICOLS-2015 (WSPC Proceedings)* arXiv:1512.01765v1 [physics.atom-ph] (6 December 2015).
[5] A1 Collaboration (Bernauer J. C. *et al.*), *Phys. Rev. Lett.*, **105** (2010) 242001.
[6] A1 Collaboration (Bernauer J. C. *et al.*), *Phys. Rev. C*, **90** (2014) 015206 (arXiv:1307.6227 [nucl-ex]).
[7] Distler M. O., Walcher T. and Bernauer J. C., *Solution of the proton radius puzzle? Low momentum transfer electron scattering data are not enough*, arXiv:1511.00479v1 [nucl-ex] (2 November 2015).
[8] Particle Data Group (Tanabashi M. *et al.*), *Phys. Rev. D*, **98** (2018) 030001 (with 2019 update).
[9] Lorenz I. T., Hammer H.-W. and Meissner U., *Eur. Phys. J. A*, **48** (2012) 151.
[10] Lorenz I. T. and Meißner U.-G., *Phys. Lett. B*, **737** (2014) 57.
[11] Griffioen K., Carlson C. and Maddox S., *Phys. Rev. C*, **93** (2016) 065207 (arXiv:1509.06676v2 [nucl-ex] (26 October 2015)).
[12] Higinbotham D. W., Kabir A. A., Lin V., Meekins D., Norum B. and Sawatsky B., *Phys. Rev. C*, **93** (2016) 055207 (arXiv:1510.01293 [nucl-ex]).
[13] Stryker J. R. and Miller G. A., *Phys. Rev. A*, **93** (2016) 012509 (arXiv:1508.06680 [hep-ph]).
[14] Bernauer J. C. and Distler M. O., *Avoiding common pitfalls and misconceptions in extraction of the proton radius*, preliminary version as discussion basis for the *ECT* workshop on The proton radius puzzle, Trento 2016*, arXiv:1606.02159v1 [nucl-th] (7 June 2016).
[15] Pohl R., Gilman R., Miller G. A. and Pachucki K., *Annu. Rev. Nucl. Part. Sci.*, **63** (2013) 175 (arXiv:1301.0905 [physics.atom-ph]).
[16] Carlson C. E., *Prog. Part. Nucl. Phys.*, **82** (2015) 59 (arXiv: 1502.05314 [hep-ph]).
[17] Sakurai J. J., *Advanced Quantum Mechanics* (Addison-Wesley, Redwood City, Cal., USA) 1967.
[18] Miller G. A., *Phys. Rev. C*, **99** (2019) 035202 (arXiv:1812.02714v1 [nucl-th] (6 December 2018)).
[19] Mihovilovic M. *et al.*, *The proton charge radius extracted from the Initial State Radiation experiment at MAMI*, arXiv:1905.11182v1 [nucl-ex] (27 May 2019).
[20] Downie E. J., *EPJ Web of Conferences*, **113** (2016) 05021.
[21] Trinhammer O. L. and Bohr H. G., *Intrinsic quantum mechanics II. Proton charge radius and Higgs mechanism*, ResearchGate, January 2017 (working paper), DOI: 10.13140/RG.2.2.32459.39209.
[22] Peset C., *Nucl. Part. Phys. Proc.*, **258-259** (2015) 231.
[23] Trinhammer O. L., Bohr H. G. and Jensen M. S., *Int. J. Mod. Phys. A*, **30** (2015) 1550078 (arXiv:1503.00620v2 [physics.gen-ph]).
[24] Trinhammer O. L., *EPL*, **102** (2013) 42002 (arXiv: 1303.5283v2 [physics.gen-ph]).
[25] Wilson K. G., *Phys. Rev. D*, **10** (1974) 2445.
[26] Kogut J. B. and Susskind L., *Phys. Rev. D*, **11** (1975) 395.
[27] Wadia S. R., *Phys. Lett. B*, **93** (1980) 403.
[28] Manton N. S., *Phys. Lett. B*, **96** (1980) 328.
[29] Trinhammer O., *Phys. Lett. B*, **129** (1983) 234.
[30] Milnor J., *Ann. Math. Stud.*, **51** (1963) 1.
[31] Trinhammer O. L., *EPL*, **124** (2018) 31001.
[32] Trinhammer O. L., *Neutron to proton mass difference, parton distribution functions and baryon resonances from*

dynamics on the Lie group $u(3)$, arXiv:1109.4732v3 [hep-th] (25 June 2012).

[33] Trinhammer O. L., *Intrinsic Quantum Mechanics Behind the Standard Model?, Proceedings of the European Physical Society Conference on High Energy Physics, EPS-HEP2019, 10–17 July, 2019, Ghent Belgium*, to be published as *PoS* (*EPS-HEP2019*) 616 at `https://pos.sissa.it`.

[34] Jacobsen Hans Plesner, *Department of Mathematics, University of Copenhagen, Denmark* private communication (approximately 1997).

[35] Schiff L. I., *Quantum Mechanics*, 3rd edition (McGraw-Hill Kogakuska, Tokyo) 1955/1968.

[36] Trinhammer O. L. and Olafsson G., *The Full Laplace-Beltrami operator on $U(N)$ and $SU(N)$*, arXiv:math-ph/9901002v2 (1999/2012).

[37] Ashcroft N. W. and Mermin N. D., *Solid State Physics* (Holt, Rinehart and Winston, New York) 1976.

[38] Trinhammer O. L., Bohr H. G. and Jensen M. S., *A Higgs at* 125.1 GeV *and baryon mass spectra from a common $U(3)$ framework, Proceedings of the European Physical Society Conference on High Energy Physics, 22–29 July 2015, Vienna, Austria*, *PoS* (*EPS-HEP2015*) 097.

[39] Weyl H., *The Classical Groups - Their Invariants and Representations*, 2nd edition (Princeton University Press) 1939 (15th printing (1997)).

[40] Nielsen H. Bruun, Technical University of Denmark, private communication (1997).

[41] Trinhammer O. L., *Intrinsic Quantum Mechanics Behind the Standard Model. From Lie group configurations to Particle Physics Observations*, ResearchGate, November 2018, `http://www.researchgate.net/publication/329587446`.

[42] Aitchison I. J. R. and Hey A. J. G., *Gauge Theories in Particle Physics - A Practical Introduction*, Vol. **2**, 4th edition (CRC Press, Boca Raton) 2013, pp. 378–379.

[43] Scheck F., *Electroweak and Strong Interactions - Phenomenology, Concepts, Models*, 3rd edition (Springer, Berlin, Heidelberg, Germany) 1996/2012, p. 240.

[44] Trinhammer O. L., *EPL*, **125** (2019) 41001.

[45] Erler J. and Schott M., *Prog. Part. Nucl. Phys.*, **106** (2019) 68 (arXiv:1902.05142v2 [hep-ph] (22 February 2019)).

[46] Heisenberg W., *Ann. Phys. (Berlin)*, **32** (1938) 20.

[47] Landau L. D. and Lifshitz E. M., *The Classical Theory of Fields, Course of Theoretical Physics*, Vol. **2**, 4th edition (Elsevier, Butterworth-Heinemann, Oxford) 2005.

[48] Weinberg S., *Lectures on Quantum Mechanics*, 2nd edition (Cambridge University Press, Cambridge, United Kingdom) 2015.

[49] Trinhammer O. L., *Neutron to proton mass difference, parton distribution functions and baryon resonances from a simple abstract model*, arXiv:1302.1779v1 [hep-ph] (7 February 2013).

[50] Messiah A., *Quantum Mechanics*, Vol. **1** (North-Holland Publishing Company, Amsterdam) 1961.